PUBLICATIONS of the EARTH PHYSICS BRANCH

VOLUME 44 – NO. 8

a three-component aeromagnetic survey of the canadian arctic

G. V. HAINES and W. HANNAFORD

DEPARTMENT OF ENERGY, MINES AND RESOURCES

OTTAWA, CANADA 1974

a three-component aeromagnetic survey of the canadian arctic

G. V. HAINES and W. HANNAFORD

Abstract. A three-component airborne magnetic survey of the Canadian Arctic was carried out in late 1970, at an average altitude of 3.7 km. The survey data are in the form of averages over 30 seconds of time, or approximately 3.5 km of flight track. The International Geomagnetic Reference Field (IGRF) was removed from these data, and the resulting residuals plotted as profiles. A 3rd-degree polynomial was fitted to the survey data by least-squares to determine how well the IGRF represents the average regional field over the area. The polynomial was also used to obtain vector residuals.

Résumé. L'arctique canadien a fait l'objet, à la fin de 1970, d'un levé magnétique aérien à trois composantes, d'une altitude moyenne de 3.7 km. Les données du levé ont la forme de périodes de plus de 30 secondes en moyenne, ou environ 3.5 km de ligne de vol. De ces données on a exclu le Champ de référence géomagnétique international (CRGI) et restitué le reste en profils. Par la méthode des moindres carrés, on a adapté un polynôme du 3^{e} degré aux données du levé pour déterminer le degré de représentation du CRGI, du champ moyen régional de la région. Le polynôme a servi également pour obtenir des résidus de vecteur.

Introduction

In 1970, between October 17 and December 11, a three-component aeromagnetic survey of the Canadian Arctic was carried out by the Earth Physics Branch, Department of Energy, Mines and Resources. An index map of the survey area is shown in Figure 1.

The aircraft used was a DC-6, chartered from Pacific Western Airlines. Approximately 93,000 line-kilometres were flown, of which about 20,000 were ferry and calibration flights. The average flight-line spacing was 74 km (40 nautical miles), and the area covered was 4.2 x 10^6 km^2. Flight altitudes ranged from 2.4 to 5.8 km above sea level, the average being 3.7 km (or 12,000 ft).

The platform, magnetometer, and data-acquisition system

The geomagnetic declination D, horizontal intensity H, and vertical intensity Z are measured by a fluxgate magnetometer with a three-component sensing head. The head is mechanically linked to a gyro-stabilized platform so as to align the H and D sensors in a horizontal plane and to hold the Z sensor axis in alignment with the vertical. Both the sensing head and the platform are pivoted on two gimbal axes that are parallel to the aircraft's roll and pitch axes. The complete assembly, shock mounted to a box-like wooden base, is shown in Figure 2.

In order to measure H and Z with an accuracy of 50 gammas or better, the instrumental system must be capable of finding the direction of the true vertical with an error less than three minutes or arc. This requirement presents a problem when the system is to operate aboard an aircraft in flight and is therefore subjected to other accelerations as well as gravity. Even under flight conditions normally considered to be steady, smooth and level, time-varying accelerations are present which will deflect the apparent vertical (level bubble) by one or two degrees. In a DC-6 aircraft flying straight and level under constant power, these perturbing accelerations vary with periods of 120 seconds or less. Over the duration of several of the longest periods involved, the net effect must of course be nil; in other words the alternating accelerations average out to zero.

Accordingly, the position of the apparent vertical is averaged over a time interval longer than any acceleration periods encountered in straight and level flight; this average is represented mechanically by the output axes of two gyros, one acting in a plane normal to the platform's pitch axis, the other acting in a roll plane. The platform is then held by servos in a plane which is normal to both gyro output axes.

More specifically, the stabilization method outlined above is implemented as follows. Accelerations in the plane of the platform are resolved in the fore-and-aft and transverse directions by two orthogonally-mounted accelerometers. The electrical analog output from each accelerometer consists of an AC component due to motions of the aircraft and possibly a DC component due to platform tilt. This output is passed through an integrator, then through an error-rate stabilization circuit, and finally applied to the torque motor of the corresponding gyro (also mounted on the platform) to precess the gyro's output axis and maintain it in the required upright position. When the platform begins to deviate from the normal plane an error signal from the appropriate gyro activates a corresponding servo to correct the incipient misalignment.

The system is designed to have a natural period of 2π minutes, and it acts as a filter to attenuate the effect of periodic accelerations which occur within the expected range of frequencies. For example, if the aircraft is subjected to an oscillation mode of acceleration which swings the apparent vertical with an amplitude of 1.0 degree and a period of one minute, the platform will respond with deflections of the same period but with an amplitude of 0.03 degree.

Better filtering could be achieved by increasing the period of the system. However, the chosen value of 2π minutes imposes a waiting time of approximately 10 minutes while the platform recovers from deflections caused by long-sustained

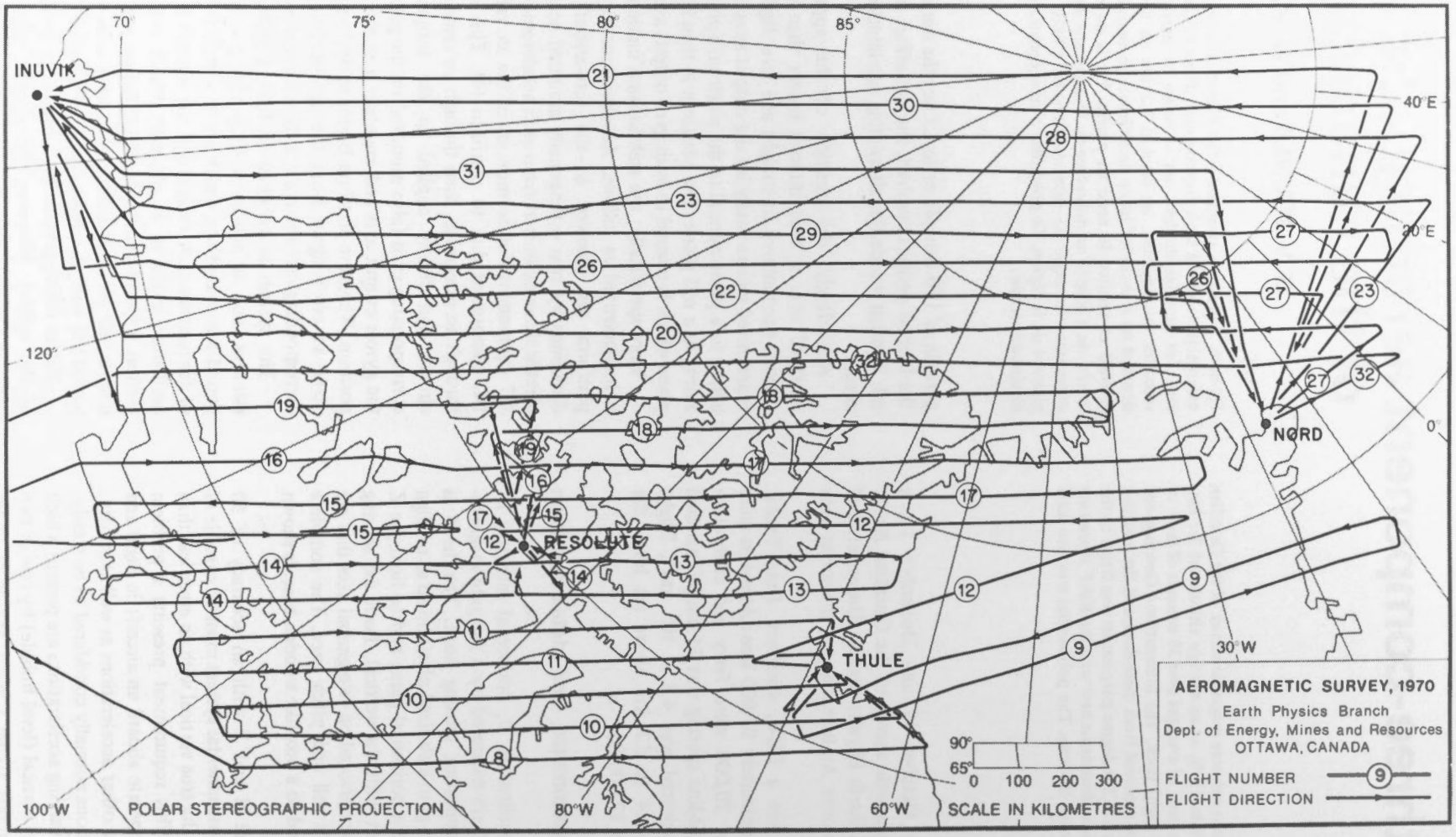

Figure 1. Flight lines of the Canadian Arctic aeromagnetic survey, 1970. Flight numbers are circled and arrowheads indicate the direction of travel.

Figure 2. The gyro-stabilized platform and fluxgate sensor assembly.

accelerations when the aircraft is climbing, descending or turning. This recovery time would also increase if the natural period of the platform was made longer, and therefore 2π minutes was chosen as the most acceptable compromise.

A third gyroscope is mounted on a turntable so that its output axis lies in a plane parallel to the platform and thus provides a directional reference for the measurement of D and of the aircraft's heading. Error signals from this gyro control a servo which drives the turntable to hold the gyro in alignment with its output axis, notwithstanding the yawing motions or turning of the aircraft.

Periodic yawing of the aircraft forces oscillations of the platform about its roll axis. To reduce these oscillations the centrifugal accelerations are computed in analog form and subtracted from the roll accelerometer signals at the input to the roll integrator. The analog computation is achieved by driving a rate generator at a speed proportional to that of the directional gyro turntable to obtain an output voltage representing the aircraft's rate of turn, and this voltage is multiplied by a factor proportional to ground speed on a servo-driven potentiometer controlled by signals from a Doppler system.

Similarly, forced oscillations about the pitch axis are reduced by differentiating the Doppler ground speed voltage (or alternatively, the output from an airspeed sensor) and, after appropriate scaling, the result is subtracted from the output of the pitch accelerometer.

A small correction to compensate for Coriolis force is also subtracted from the roll accelerometer output.

As the earth rotates at a rate of 15° per hour, the horizontal component of this rotation, at latitude θ, is $15^\circ \cos\theta$ per hour. In the two planes normal to the pitch and roll axes this rate is resolved according to the true heading of the aircraft and corresponding precession torques are applied to the pitch and roll gyros. The latitude factor is manually set and a sine-cosine resolver automatically follows the aircraft's heading to produce the desired precession torques in pitch and roll. Thus the controlled precession rate of both vertical gyros is continously adjusted while the aircraft is making a turn, to avoid the transient which would otherwise occur because of an intolerable lag in the control exercised by the accelerometers alone.

A synchro-servo system drives the horizontal circle of a periscopic sextant to follow the rotation of the directional gyro turntable with respect to the aircraft. The angle in azimuth between the directional gyro's reference axis and an astronomical body is thus indicated. Several sextant observations are made after each 15- to 20-minute interval, to determine the gyro's true azimuth and drift rate. If necessary, the drift rate is adjusted to keep it below 2 degrees per hour.

The periscopic sextant is hung in a stabilized mount which is driven by pitch and roll synchro-servo systems to follow the attitude of the platform.

The three fluxgate sensors are orthogonally mounted at the centre of an orthogonal pair of field-cancelling coils; one for Z and the other for H. The sensing head is seen in Figure 2 at the far end of a $2\frac{1}{2}$-inch diameter horizontal shaft. It is this shaft which transmits rotation from the roll gimbal of the platform to the sensors. The same shaft and roll gimbal also form the top side of a parallelogram. The bottom side is an aluminum connecting rod which transmits the pitch motion from the lower end of a downward arm on the platform (front side of the parallelogram) to the lower end of the sensor assembly (rear side). The sensor assembly consists of the sensing head, which is rotated in azimuth at the top end of a vertical shaft and, at the opposite end of this shaft, a servo drive controlled by the output of the D fluxgate to hold it at a null. Consequently the H fluxgate and field-cancelling coil are aligned with magnetic north.

In an area around the magnetic pole where H is diminished to approximately the same magnitude as the horizontal component of the aircraft's magnetic field, their vector sum may become small enough to keep the D fluxgate's error signal output below the noise level. Under such conditions there is no control on the azimuthal alignment of the sensing head; the observed D becomes indeterminate and the measurement of H is invalid. Since the north magnetic pole is in the area covered by the survey which is the subject of this report, pre-survey tests were made under conditions simulating low values of H. As the simulated H was reduced during these tests, the sensing-head servo would become sluggish and the accuracy of alignment was severely degraded before a useful D error signal was lost. This problem was removed by introducing a circuit whereby the voltage gain of the sensing-head servo is made inversely proportional to H and thus the overall gain of the system remains constant. As a result the sensing-head orientation remained stable over the full range of H, except for a few very brief periods in the immediate area of the pole. The longest of these lapses covered approximately 15 kilometres of a flight line.

Figure 3 is a simplified schematic diagram of the magnetometer and data-acquisition system. The azimuth angle between the H-axis of the sensing head and the directional gyro is transmitted via synchrosignals to a servo-driven potentiometer which produces the voltage analog. This voltage is continuously recorded and later converted to D when the azimuth-vs-time curve of the directional gyro is determined with final accuracy.

During the survey an unforseen problem arose at very high geomagnetic latitudes where local anomalies may cause a very large change in D. Under these circumstances the top speed of the servo driving the D-analog potentiometer was sometimes inadequate for following the rapid change and, because of the gear ratios involved, the potentiometer would suddenly lag by 10 degrees. It was sometimes impossible to determine the number of 10-degree lags which occurred when they came in rapid succession, and in such cases a section of D information was lost.

The feedback currents which cancel the field inside the H and Z coil systems are passed through precision resistors, giving DC voltages proportional to the horizontal and vertical components of the magnetic field.

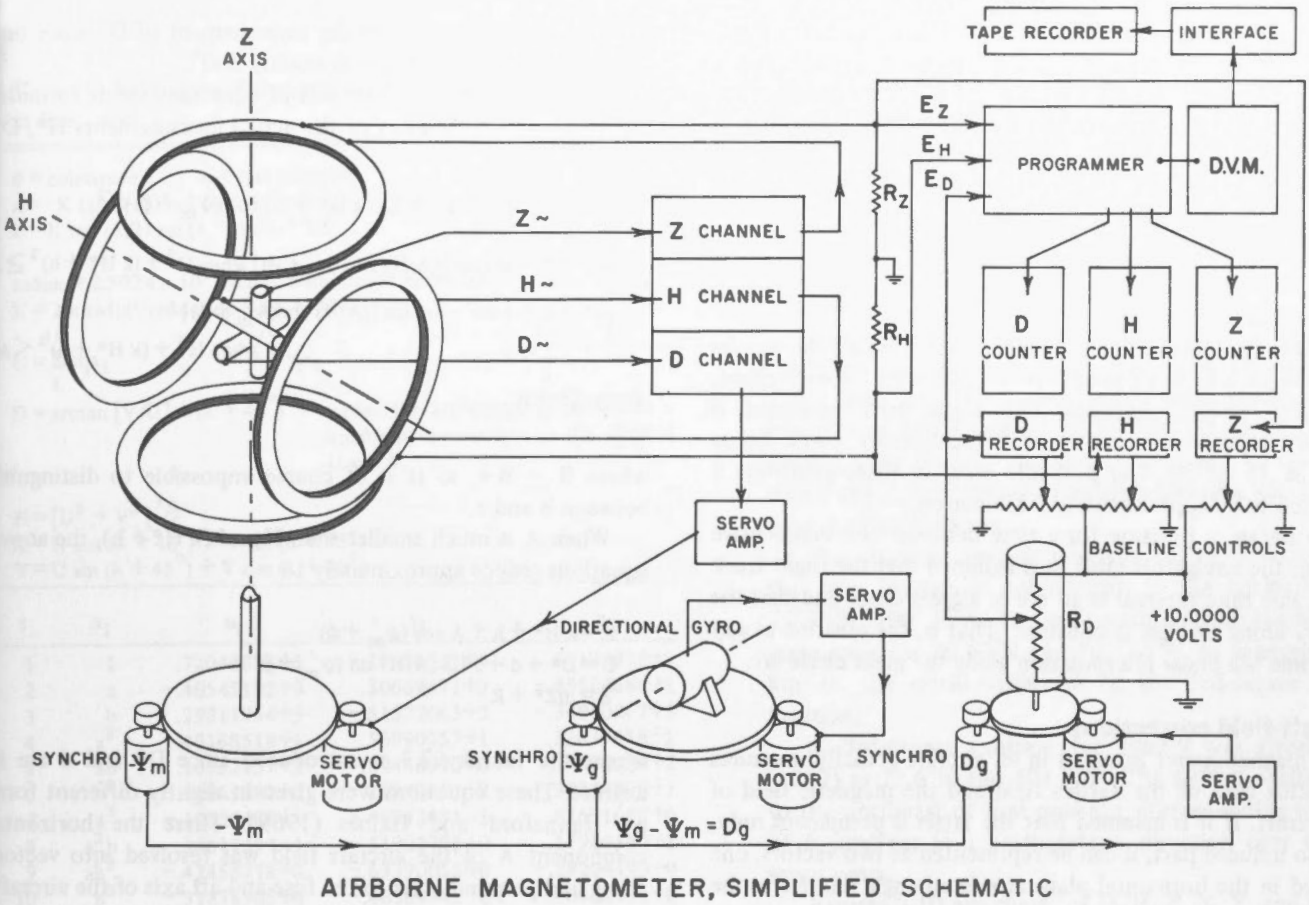

AIRBORNE MAGNETOMETER, SIMPLIFIED SCHEMATIC

Figure 3. Simplified schematic of the magnetometer and data-acquisition system.

The three components D, H, and Z are recorded in both analog and digital form. For analog recording, each of the three voltages is fed directly to a strip chart recorder. The records are kept on scale by manually selecting an appropriate reference voltage from a very accurate incremental voltage divider.

For digital recording, the three voltages are fed into a clock-controlled programmer unit, which switches from D to H to Z every 3 seconds. Thus, the digital voltmeter (D.V.M.) measures D, H, and Z 20 times per minute, and outputs this to a magnetic tape recorder. At the end of every minute, the programmer also sends to the tape recorder digital signals representing the year, month, day, and universal time.

The programmer unit also channels pulses from the D.V.M. into three counters, and accumulates these pulses for 5 minutes. At the end of the 5-minute period the counters display the accumulated pulse count. This can be read as a 5-minute average by a simple shift of decimal point since there are 20 x 5 = 100 measurements in the 5-minute interval. These 5-minute averages are written down by the operator and can be used in the event of tape-recorder or strip-chart recorder failure.

In addition to the DHZ fluxgate magnetometer, the aircraft carries a proton-precession magnetometer which makes a measurement of total magnetic intensity F, every three seconds. These measurements are synchronized with the digital sampling of D, H, and Z and are recorded on the same magnetic tape. They are also converted to analog form and recorded on a strip-chart. The sensing head of the proton magnetometer is mounted at the end of a "stinger", or long hollow boom, attached to the rear of the aircraft. The stinger extends about 3.5 metres from the end of the fuselage. Unfortunately, the proton magnetometer did not work well during this survey, and was used mainly as a cross-check of the fluxgate measurements.

The design of the stabilized platform, fluxgate magnetometer, and mechanical linkage system has been described in detail by Serson *et al.* (1957). The magnetometer and data-acquisition system was re-designed in 1965, and described by Hannaford *et al.* (1967).

Navigation

Two navigators, supplied as part of the air crew by the charter company, were on duty at all times during flights. The company was required to fly 22 lines at a spacing of 40 nautical miles (74 km) and on grid headings of 135 and 315 degrees. (Grid heading is true heading plus west longitude; on a polar stereographic map it is the clockwise angle from the 180° meridian to the direction of flight.)

The aircraft was fitted with a Marconi Doppler unit, Model CMA621-A, which measures ground speed and drift, and a Doppler computer, Model CMA601, to calculate the distance travelled along and perpendicular to a given track. This track is selected with respect to the directional gyro on the stabilized platform.

Other navigational aids were the standard ones of visual map checks ("pinpoints"), observations on astronomical bodies, radar fixes (bearing and distance from a radar station) and position information from Loran stations.

After the survey, the navigators back-plot all the results and produce a table of positions and altitudes for each flight. The time interval between two consecutive positions is generally around 10 minutes, but occasionally could be as much as 15 or 20. The probable error in these positions is estimated to be approximately 5 kilometres.

To obtain a position for a time between two consecutive times in the navigators table, it is assumed that the flight track during this time interval is an arc of a great circle and that the velocity along this arc is constant. That is, the position at any given time is a linear interpolation along the great circle arc.

Aircraft-field corrections

A magnetometer installed in an aircraft actually measures the vector sum of the earth's field and the magnetic field of the aircraft. If it is assumed that the latter is permanent only, with no induced part, it can be represented as two vectors, one oriented in the horizontal plane at a fixed angle relative to the aircraft and one in the direction of the vertical.

Suppose the horizontal component of the aircraft field is represented as a vector of magnitude A oriented at an angle ϕ with respect to the fore-and-aft axis of the aircraft. Let the declination, horizontal, and vertical components of the earth's field be denoted by D, H, and Z, respectively, and of the apparent field (earth's plus aircraft field) by D′, H′, and Z′. If the apparent magnetic heading (the clockwise angle from the H′ vector to the aircraft's fore-and-aft axis) is denoted by ψ'_m, we have that

$$H = [H'^2 + A^2 + 2AH' \cos(\Psi'_m + \phi)]^{1/2}$$

$$D = \begin{cases} D' + \arcsin[(A/H)\sin(\Psi'_m + \phi)] & \text{when } H^2 + H'^2 \geq A^2 \\ D' + 180^\circ - \arcsin[(A/H)\sin(\Psi'_m + \phi)] & \text{when } H^2 + H'^2 < A^2 \end{cases}$$

$$Z = Z' + B$$

where the principal arc sine is used, lying between -90° and $+90^\circ$. Note that for a solution of D, it is necessary to have H and hence H′. The correction B comes from the vertical component of the aircraft field, and is independent of aircraft heading.

Now, measurements of the vectors H′, D′, and Z′ are subject to calibration errors in the measuring equipment, and so these vectors can be written

$$H' = k H^* + h$$
$$D' = D^* + d$$
$$Z' = m Z^* + z$$

There is no scaling error in the measurement of D′, since one revolution of the D-fluxgate is exactly 360°.

Combining the last two sets of equations yields formulas for H, D, and Z in terms of the actual measurements H*, D* and Z*:

$$H = [(k H^* + h)^2 + A^2 + 2A(k H^* + h)\cos(\Psi'_m + \phi)]^{1/2}$$

$$D = \begin{cases} D^* + d + \arcsin[(A/H)\sin(\Psi'_m + \phi)] & \text{when } H^2 + (k H^* + h)^2 \geq A^2 \\ D^* + d + 180^\circ - \arcsin[(A/H)\sin(\Psi'_m + \phi)] & \text{when } H^2 + (k H^* + h)^2 < A^2 \end{cases}$$

$$Z = m Z^* + R$$

where R = B + z. It is of course impossible to distinguish between B and z.

When A is much smaller than H and (k H* + h), the above equations reduce approximately to

$$H = k H^* + h + A\cos(\psi'_m + \phi)$$
$$D = D^* + d + 57.3\,(A/H)\sin(\psi'_m + \phi)$$
$$Z = mZ^* + R$$

where the factor 57.3 is introduced since D* and d are in degrees. These equations were given in slightly different form by Hannaford and Haines (1969). There the horizontal component A of the aircraft field was resolved into vectors along and perpendicular to the fore-and-aft axis of the aircraft.

To correct the magnetic measurements D*, H*, and Z*, it is necessary to know A, ϕ, R, k, h, m, and d. To determine these constants, flights are made over a point where the earth's field is very accurately known. The constants are then determined by least-squares, after the D-values are weighted as H (the equation for D is multiplied by H/57.3 if D is in degrees). Of course, the equations are non-linear in the unknowns and so an iteration method must be used to minimize the residual mean square. The results for this survey are A = 242γ, $\phi = -95^\circ$, h = 11γ, d = 2.0°, R = 374γ, where k and m were taken to be exactly 1, since the least-square solution for each was found to be not significantly different from 1.

The main field

The magnetic data were reduced to sea-level by the "inverse-cube" relationship, where it is assumed that a component P diminishes as $1/r^3$, r being the distance from the centre of the earth to the point of observation. The derivative of P then diminishes as 3P/r, and the correction to P for a change in altitude of h kilometres is given by

$$\Delta P = 4.6 \times 10^{-4}\, P h .$$

By the method of least-squares, 3rd-degree polynomials in each of three orthogonal components were then obtained by using every tenth $\frac{1}{2}$ minute average in the survey area. The resulting coefficients and the formulae for their use are given in Table I.

Table I. 3rd-Degree Polynomial Reference Field for 1970.9, at Sea Level

θ = colatitude λ = east longitude
$a = -K \tan(\theta/2) \cos(\lambda + 45^\circ) + 5.5$
$b = K \tan(\theta/2) \sin(\lambda + 45^\circ) + 5.5$

radius = 2.5024×10^8 inches; reduction = 6,000,000
$K = 2 \times$ radius/reduction = 83.41333

$$U = \sum_1^{10} u_i x_i \qquad V = \sum_1^{10} v_i x_i \qquad Z = \sum_1^{10} z_i x_i$$

$D = \arctan[V/U] + (\lambda + 45^\circ)$ where the arctangent is chosen in a quadrant appropriate to the signs of U and V.

$H = [U^2 + V^2]^{1/2}$
$X = U \cos(\lambda + 45^\circ) - V \sin(\lambda + 45^\circ)$
$Y = U \sin(\lambda + 45^\circ) + V \cos(\lambda + 45^\circ)$

i	x_i	u_i	v_i	z_i
1	1	.72043887+3	-.15436631+4	.57138975+5
2	a	-.40545122+3	.30669471+3	-.85584689+1
3	b	.29811754+3	-.51372663+3	-.34020267+3
4	a^2	.40168518+1	.56890757+1	.32637618+1
5	ab	.16752137+2	.84448970+0	.27592084+2
6	b^2	-.41661182+0	.10843077+2	-.30234890+1
7	a^3	-.10335480+1	-.49953631-3	.61591658+0
8	a^2b	.38611397-1	-.51902791+0	.17989560+1
9	ab^2	-.42458778+0	-.63390055+0	-.28204490+0
10	b^3	-.31818905+0	-.48364142+0	.40652571+0

Note: Coefficients are in floating point notation, a decimal fraction followed by a power of ten.

The standard deviations of the least-squares fit for 1st, 2nd, 3rd, and 4th degree polynomials are given in Table II. It can be seen that there is a considerable reduction in the standard deviations in going from the 2nd to 3rd degree, but very little in going on to the 4th degree. The component V is in the direction of the "x-axis" of the maps, or from left to right, and the component U is in the direction of the "y-axis", or from the bottom to the top of the maps.

The International Geomagnetic Reference Field (IGRF) is an 8th order spherical harmonic reference field adopted by the International Association of Geomagnetism and Aeronomy in 1969. The differences between components computed from the 3rd-degree polynomials of Table I and those from the IGRF are shown in Figure 4. It can be seen that there are large biases in the IGRF, as was found on a previous survey (Haines and Hannaford, 1972). In the case of Z there is a feature, parallel to and just north of the Arctic mainland, of approximately 2,000 km wavelength and about 150γ amplitude.

Table II. Standard Deviations of the Observed Minus Polynomial Field, for 1st, 2nd, 3rd, and 4th Degree Polynomials. Sample size = 1495 (every tenth $\frac{1}{2}$ minute average).

Degree	Coefficients	U	V	Z
1	3	290.8γ	322.5γ	499.1γ
2	6	152.4	154.8	172.9
3	10	139.3	124.1	147.7
4	15	136.0	124.0	143.9

Note: $U = H \cos[D - (\lambda + 45^\circ)]$ and $V = H \sin[D - (\lambda + 45^\circ)]$. The polynomials are in the two variables a and b defined in Table I.

It is also striking that the vertical field increases by about 300γ when coming onto the Canadian Shield from the Arctic Ocean and Sverdrup Basin. This is quite vividly displayed in Figure 2 of Riddihough *et al.* (1973). The same characteristic appears over British Columbia (Haines and Hannaford, 1972) where the Z field over the Canadian Shield is 400γ higher than over the Pacific Ocean.

The magnetic dip pole position (for 1970.9) obtained from the two 3rd-degree polynomials in the horizontal plane is 75°53'N, 100°23'W. The pole position from the IGRF for the same epoch is 76°45'N and 101°45'W, or approximately 100 km to the north-northwest of the 3rd-degree polynomial position.

A 3rd-degree position for 1963.9 was given by Haines (1967) as 75.6°N and 101.3°W. The 1970.9 position is 40 km to the northeast of that position, corresponding to a drift rate of 6 km/year in a northeasterly direction over the previous seven years.

Figures 5-10 are charts of D, H, Z, X, Y, and F computed from the polynomial of Table I. The corresponding pole position is shown on the D, H, X, and Y maps.

The anomaly field

Notwithstanding the large biases in the IGRF, as indicated by Figure 5, this reference field was still used in plotting residual profiles (Figures 11-15). This is because the IGRF is an international standard, with which most countries are now familiar and which provides a standard method for presentation of short-wavelength or anomaly fields.

The residuals are the observed values (corrected of course for aircraft fields) minus the corresponding IGRF values at the altitude of observation. They are plotted toward the top of the map when positive and toward the bottom when negative.

Since residual declination values in areas close to the pole are very sensitive to the main-field pole position, the 100-km error in the IGRF pole position distorts the true D-anomaly field in these areas. The effect, in Figure 11, is the appearance of large positive anomalies west of the magnetic pole and large negative anomalies east of the pole. When the 3rd degree polynomial of Table I is subtracted for the observations, the anomaly field shown in Figure 16 results. Here the distorting effect of the IGRF pole position has been removed, and the result is a clearer indication of the validity of compass readings in the Arctic area.

The anomaly field can also be represented in vector form. In order that this form of representation bear any significance,

however, it is necessary that the reference field fit the data well enough that the residuals have nearly zero mean. Hence for computing vector residuals, the 3rd degree polynomial was again used. Vector residuals in the horizontal plane are shown in Figure 17. Those in a vertical plane through the "x-axis" of the map are rotated 90° about this axis and plotted in Figure 18. (The "x-axis" is the axis of almost all the flight lines in the diagram.) Components of these two-dimensional vectors are plotted to the top and right of the map when positive, to the bottom and left when negative.

A contoured Z-residual map has been published by Riddihough *et al.* (1973). It was derived mainly from Figure 13 but also uses some data from two previous (1963 and 1965) aeromagnetic surveys over the same area. The authors discuss the major tectonic features of the area, and relations between the Canadian Shield, the Innuitian Region, and the oceanic ridges of the Arctic Basin.

Acknowledgments

The authors wish to thank Dr. P.H. Serson for his help and guidance, and for reviewing the manuscript.

The data were collected by Earth Physics Branch personnel F. Andersen, G.L. Carr, and the authors.

References

Haines, G.V. 1967. A Taylor expansion of the geomagnetic field in the Canadian Arctic. *Pub. Dom. Obs.*, Vol. XXXV, No. 2, 115-140.

Haines, G.V. and W. Hannaford. 1972. Magnetic anomaly maps of British Columbia and the adjacent Pacific Ocean. *Pub. Earth Phys. Br.* 42, No. 7, 211-228.

Hannaford, W. and G.V. Haines. 1969. A three-component aeromagnetic survey of the Nordic countries and the Greenland Sea. *Pub. Dom. Obs.*, Vol. XXXVII, No. 5, 113-164.

Hannaford, W., F. Andersen and P.H. Serson. 1967. A new three-component airborne magnetometer. Geomagnetic Report No. 67-3, Earth Physics Branch, Dept. Energy, Mines and Resources, Canada. (Abstract only, *IAGA Bull.* No. 24, p. 48, Paris, 1967.)

International Association of Geomagnetism and Aeronomy, Commission 2, Working Group 4, 1969. International Geomagnetic Reference Field 1965.0 *J. Geophys. Res.* 74, No. 17, 4407-4408.

Riddihough, R.P., G.V. Haines and W. Hannaford. 1973. Regional magnetic anomalies of the Canadian Arctic. *Can. J. Earth Sci.* 10, No. 2, 157-163.

Serson, P.H., S.Z. Mack and K. Whitham. 1957. A three-component airborne magnetometer. *Pub. Dom. Obs.*, Vol. XIX, No. 2, 15-97.

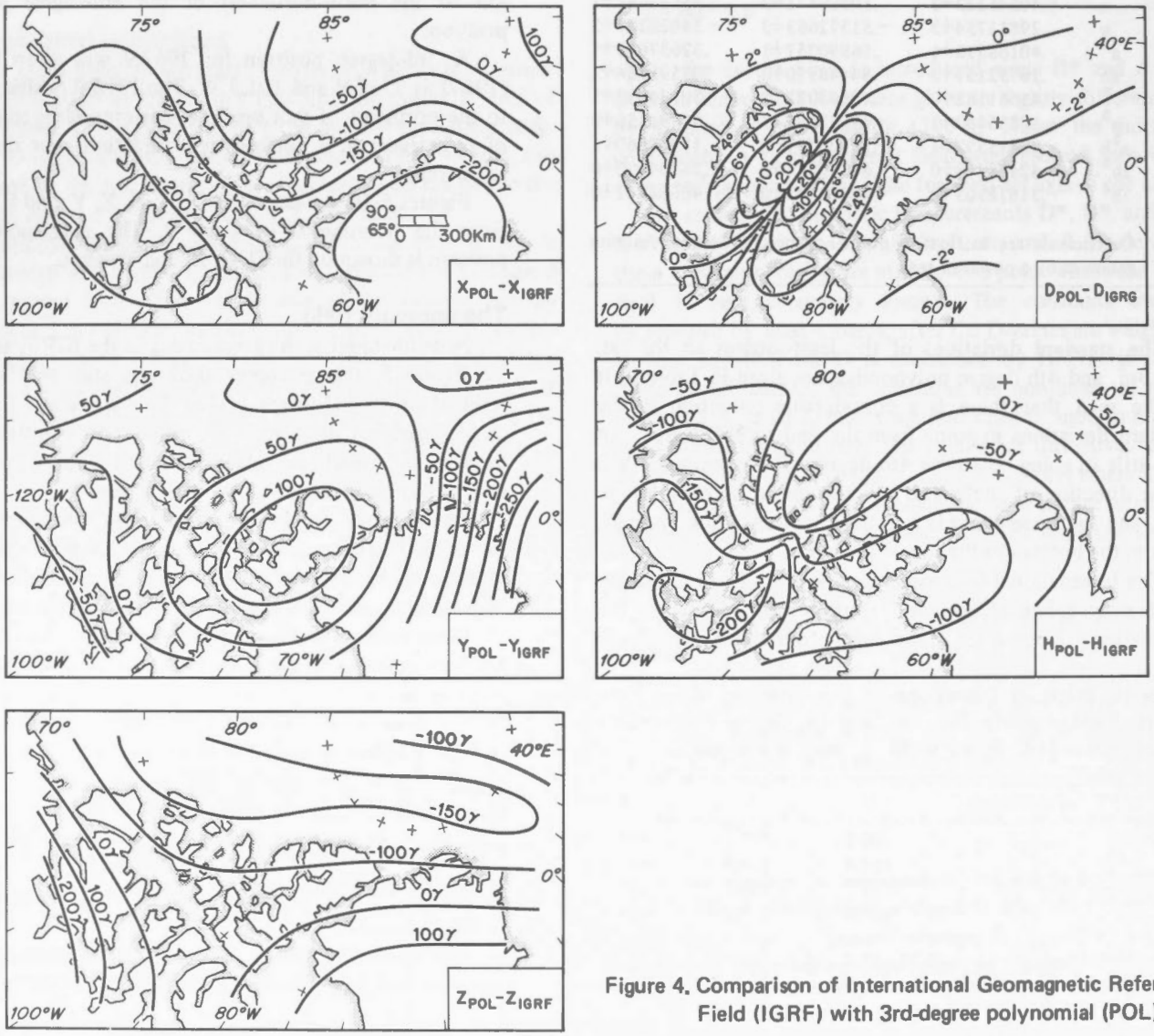

Figure 4. Comparison of International Geomagnetic Reference Field (IGRF) with 3rd-degree polynomial (POL).

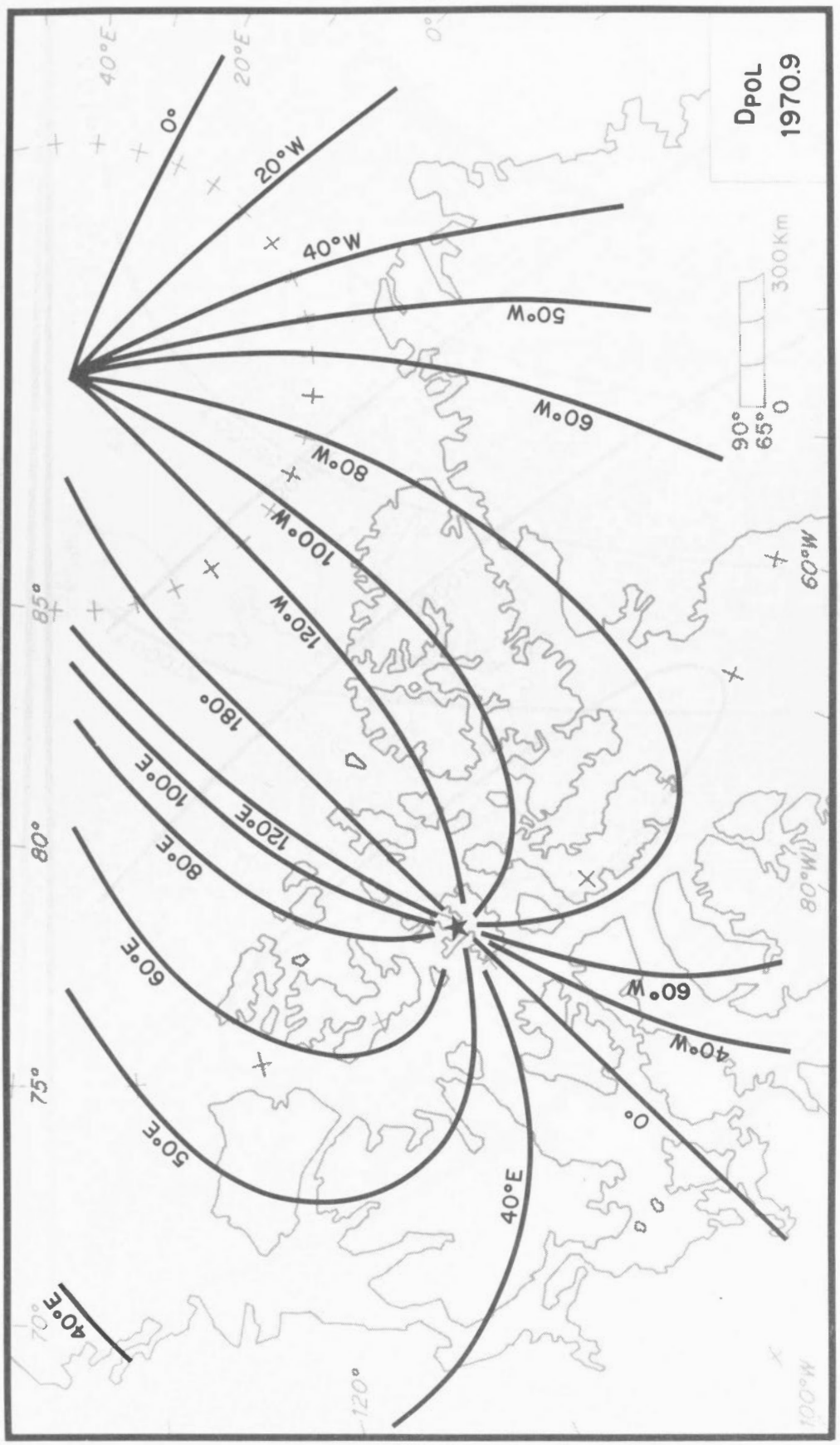

Figure 5. Declination D from 3rd-degree polynomial. Dip pole position from this polynomial is indicated by a star.

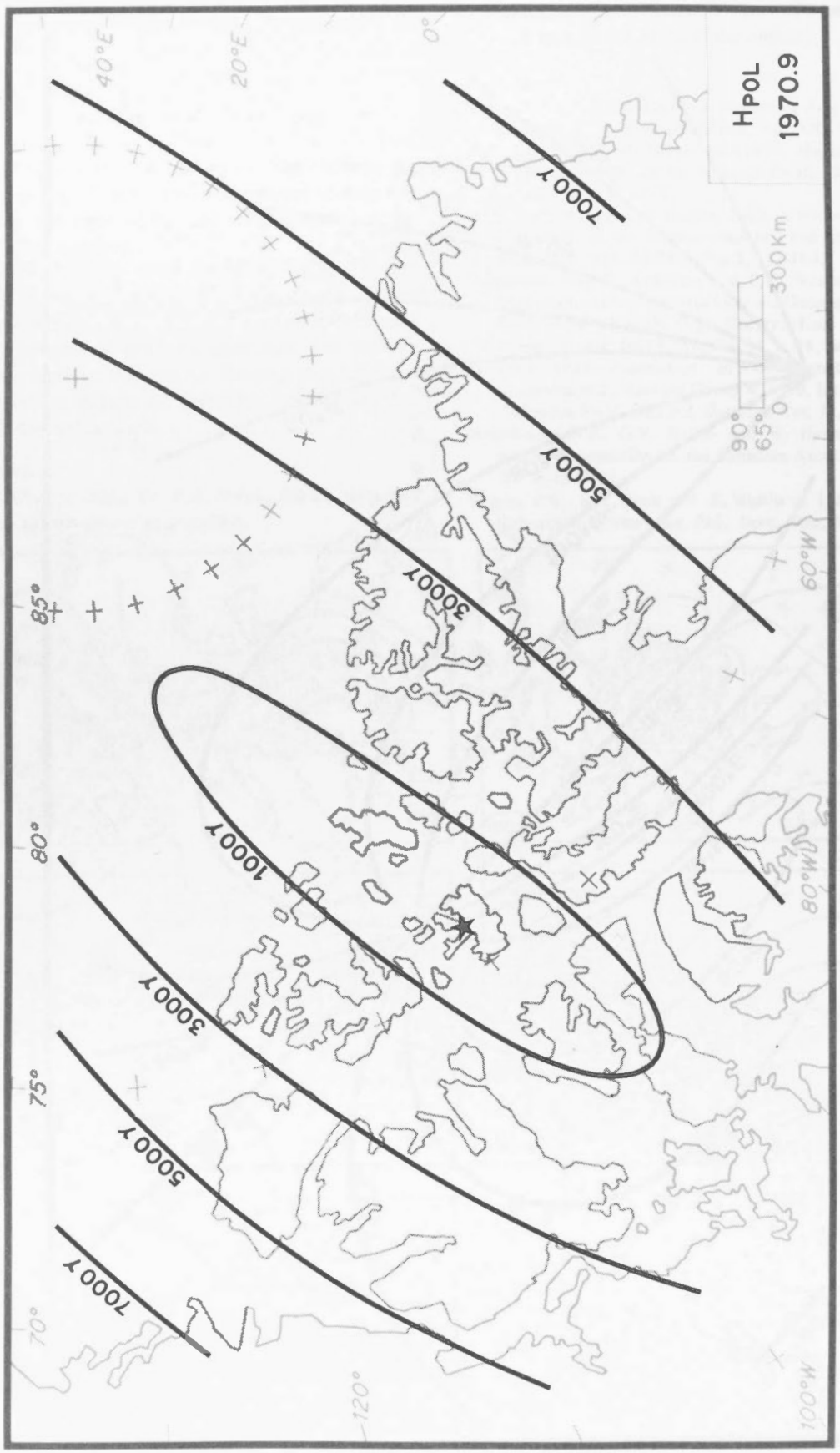

Figure 6. Horizontal intensity H from 3rd-degree polynomial.

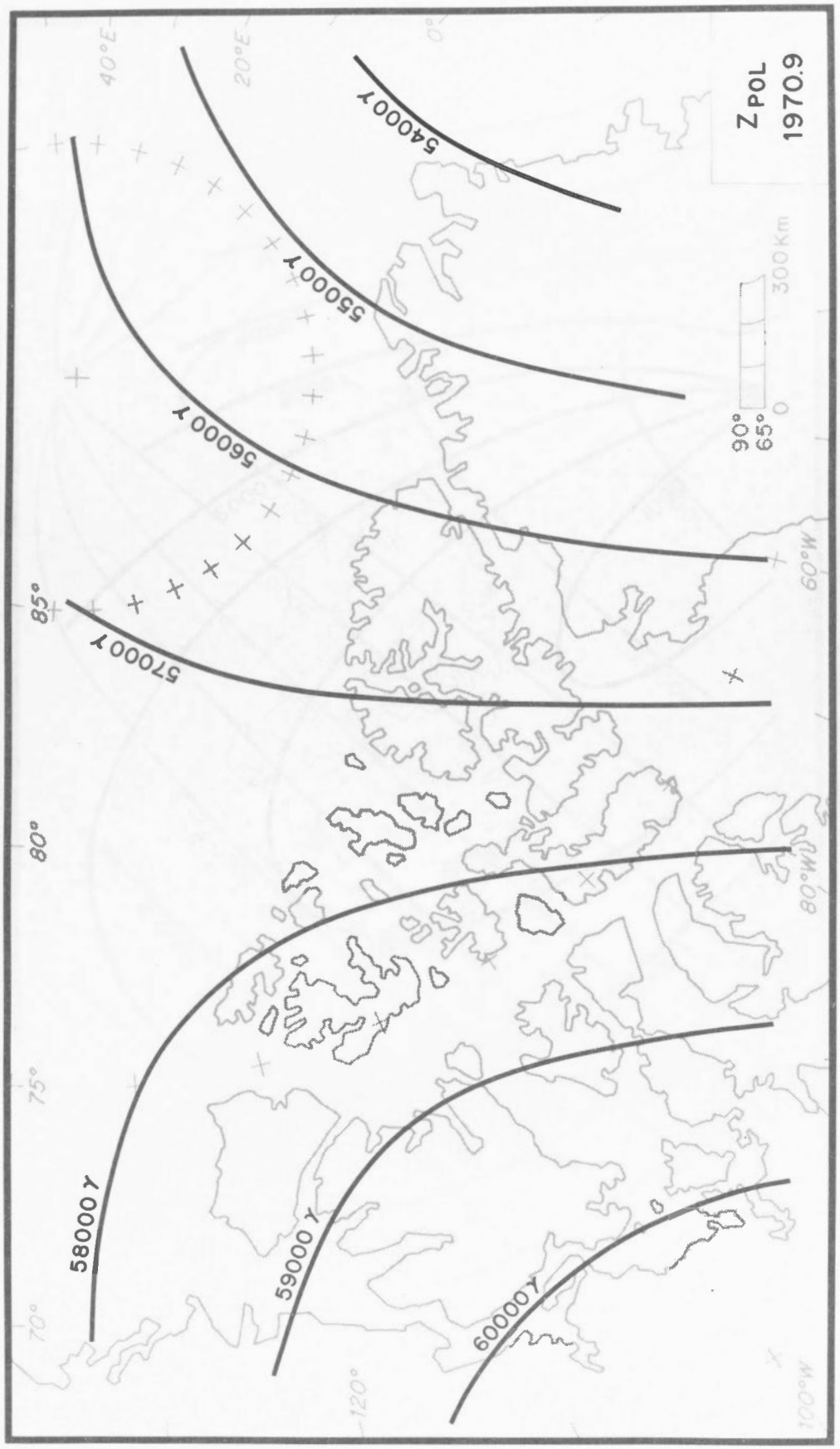

Figure 7. Vertical intensity Z from 3rd-degree polynomial.

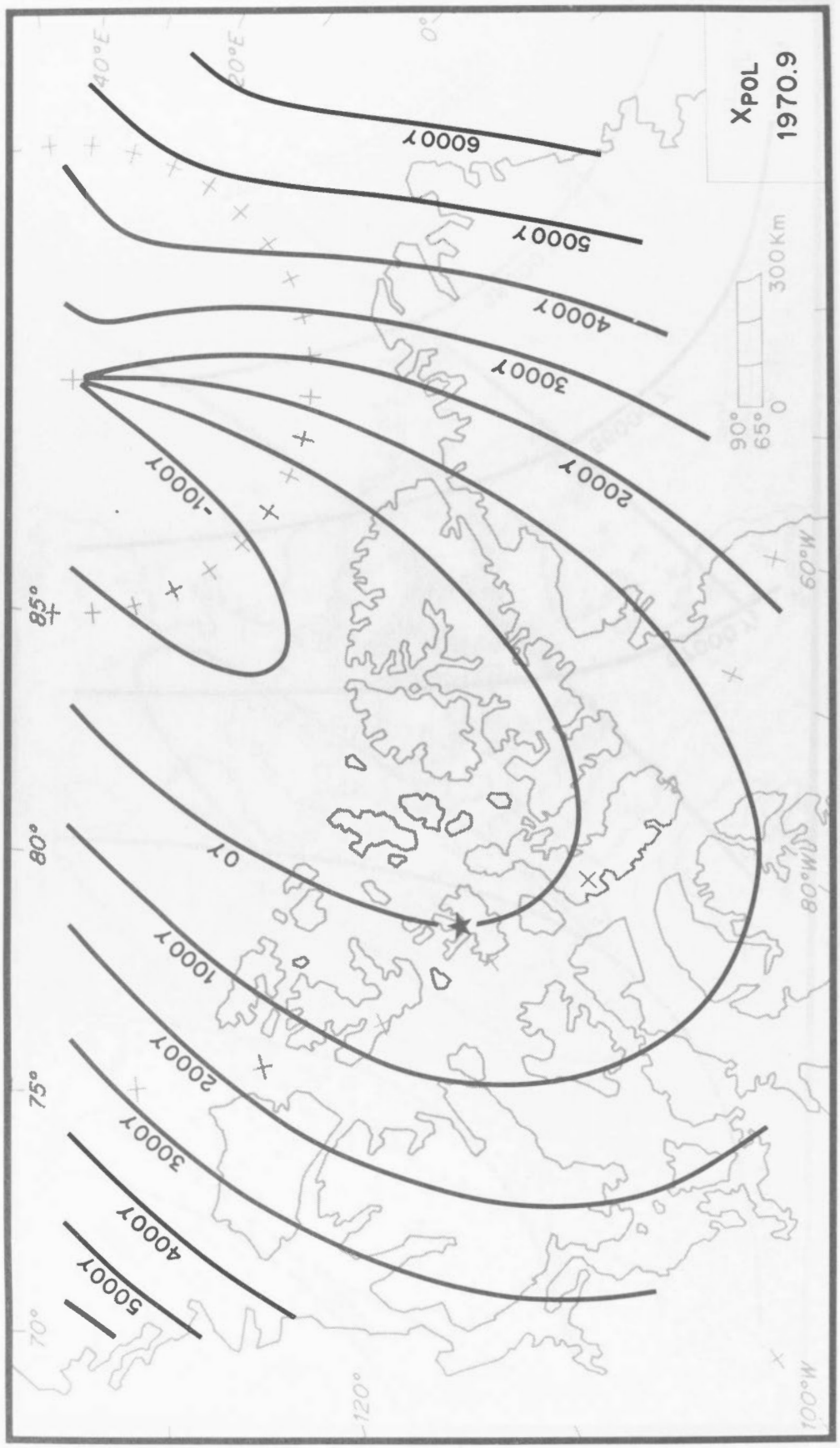

Figure 8. Geographic north component X from 3rd-degree polynomial.

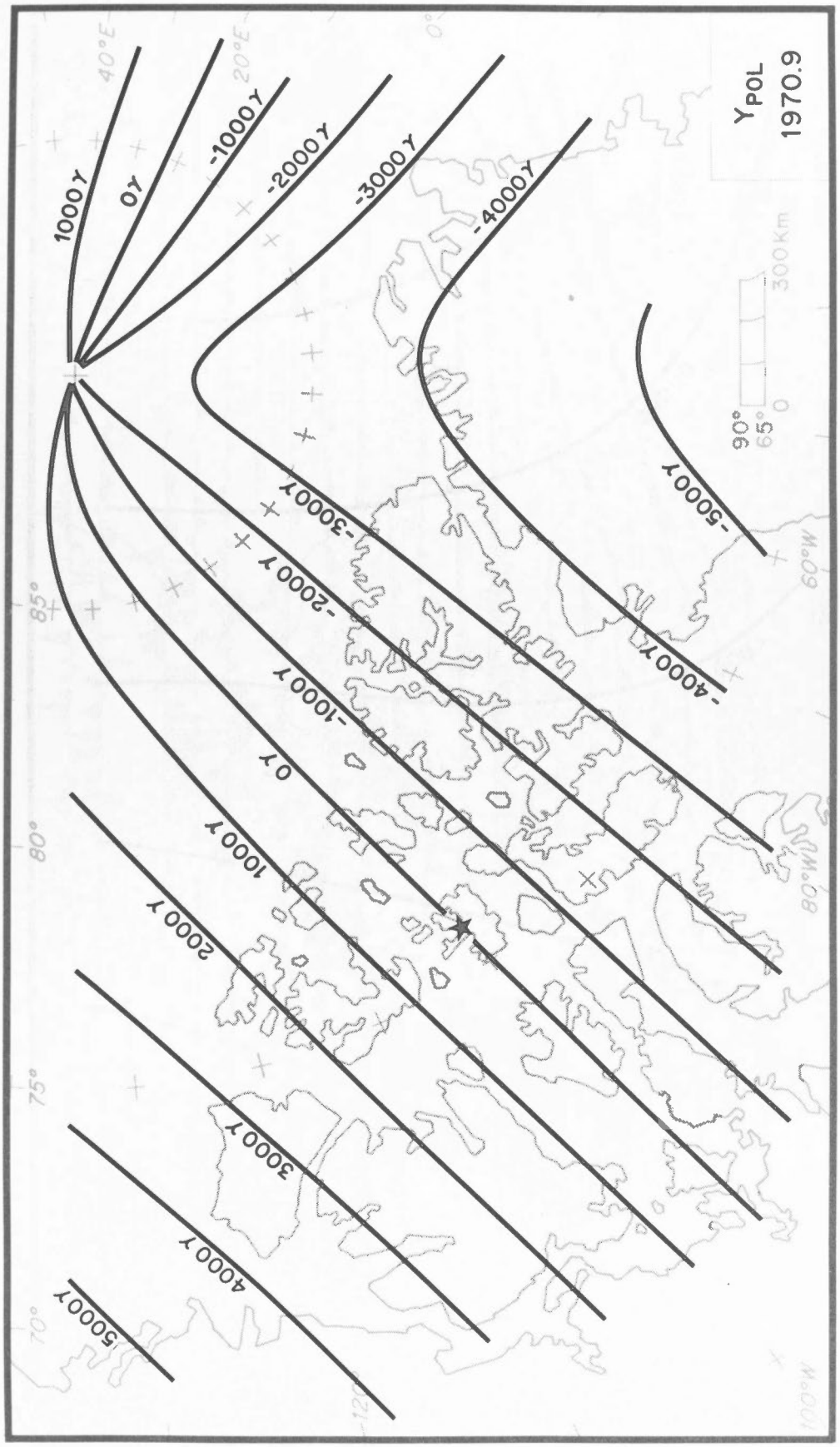

Figure 9. Geographic east component Y from 3rd-degree polynomial.

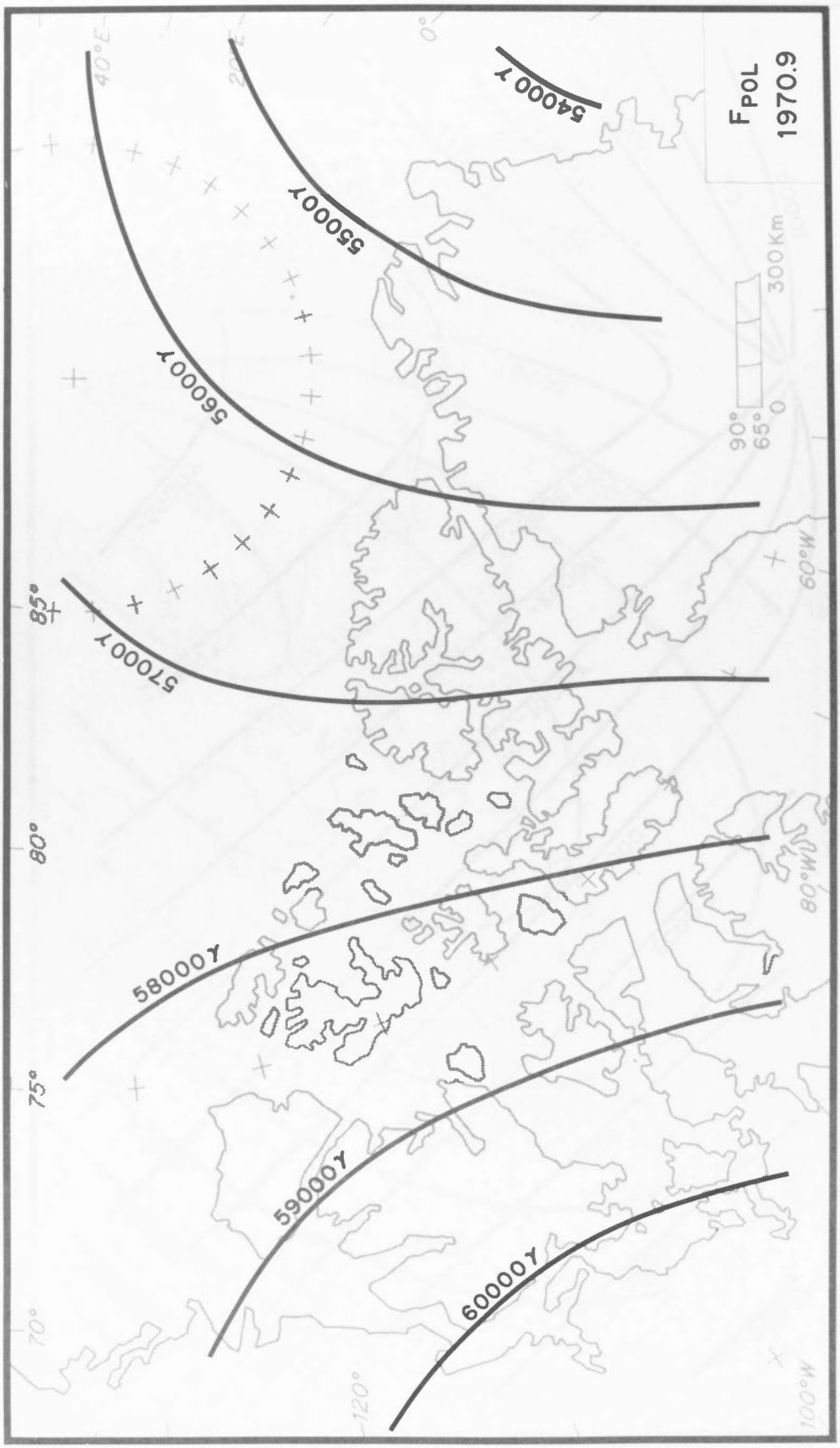

Figure 10. Total field F from 3rd-degree polynomial.

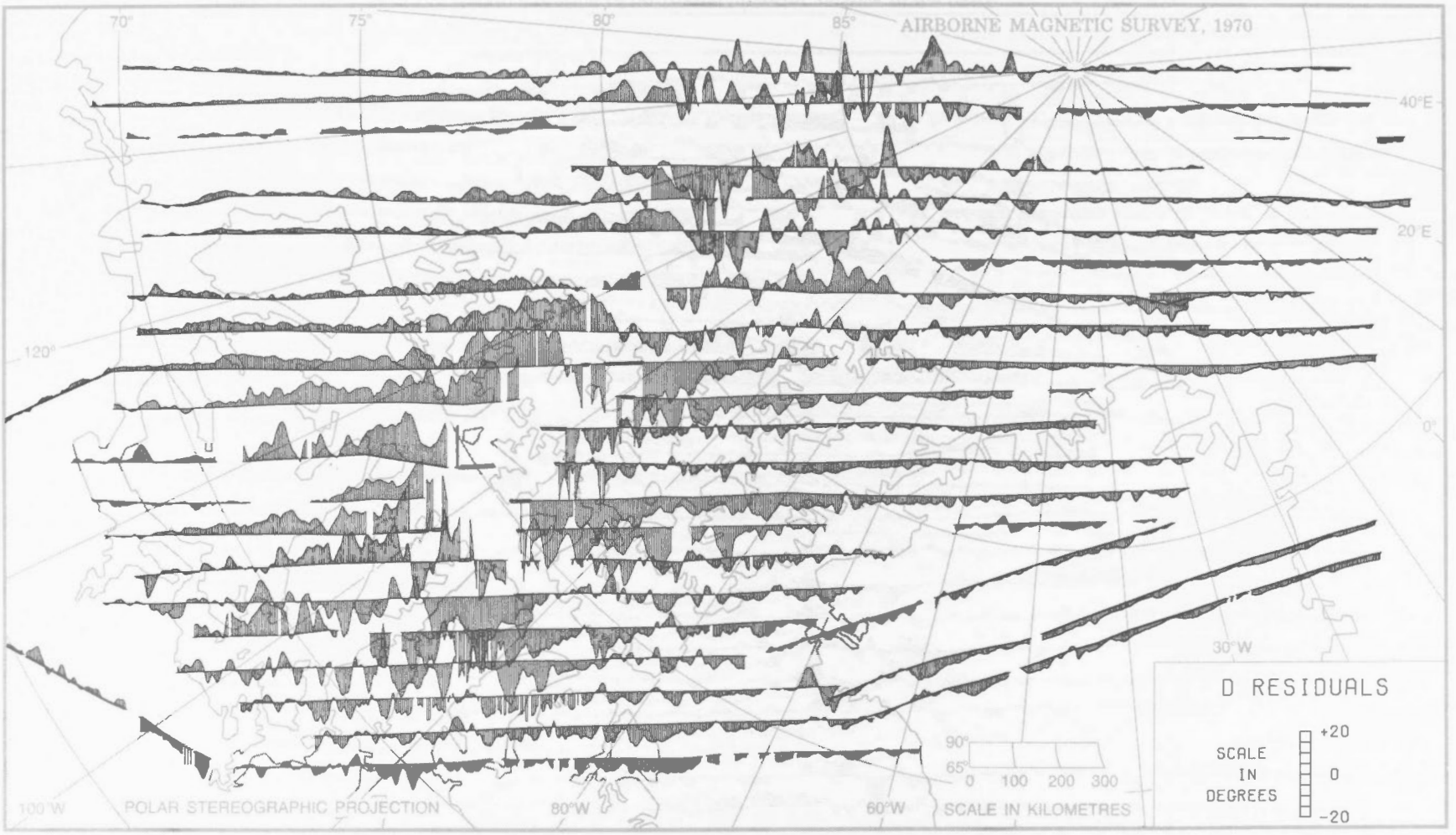

Figure 11. Residual profiles of declination, relative to the International Geomagnetic Reference Field (IGRF). A residual is an observed value minus the reference field value. Positive residuals are plotted toward the top of the map, negative toward the bottom.

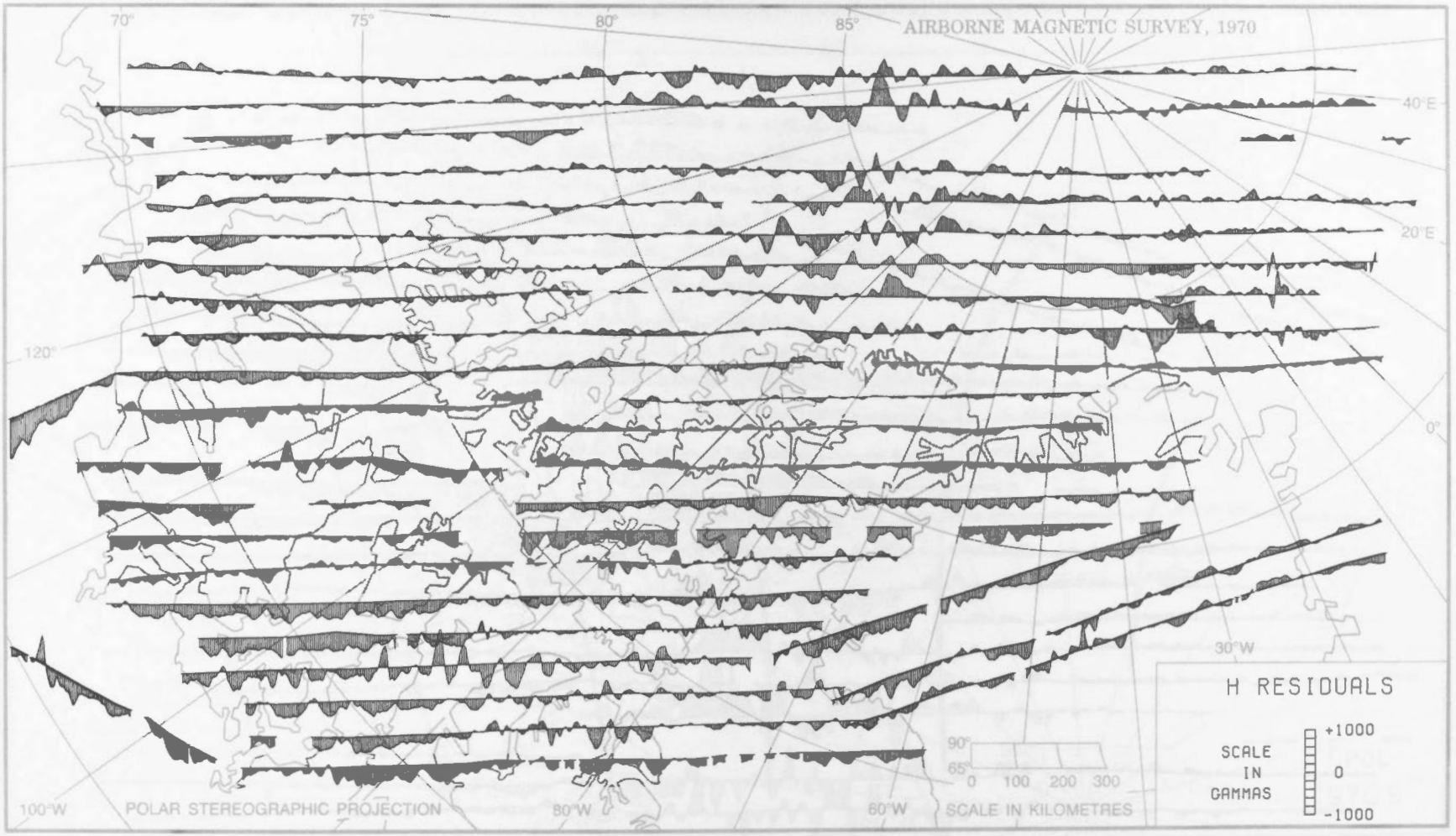

Figure 12. Residual profiles of horizontal intensity, relative to the IGRF.

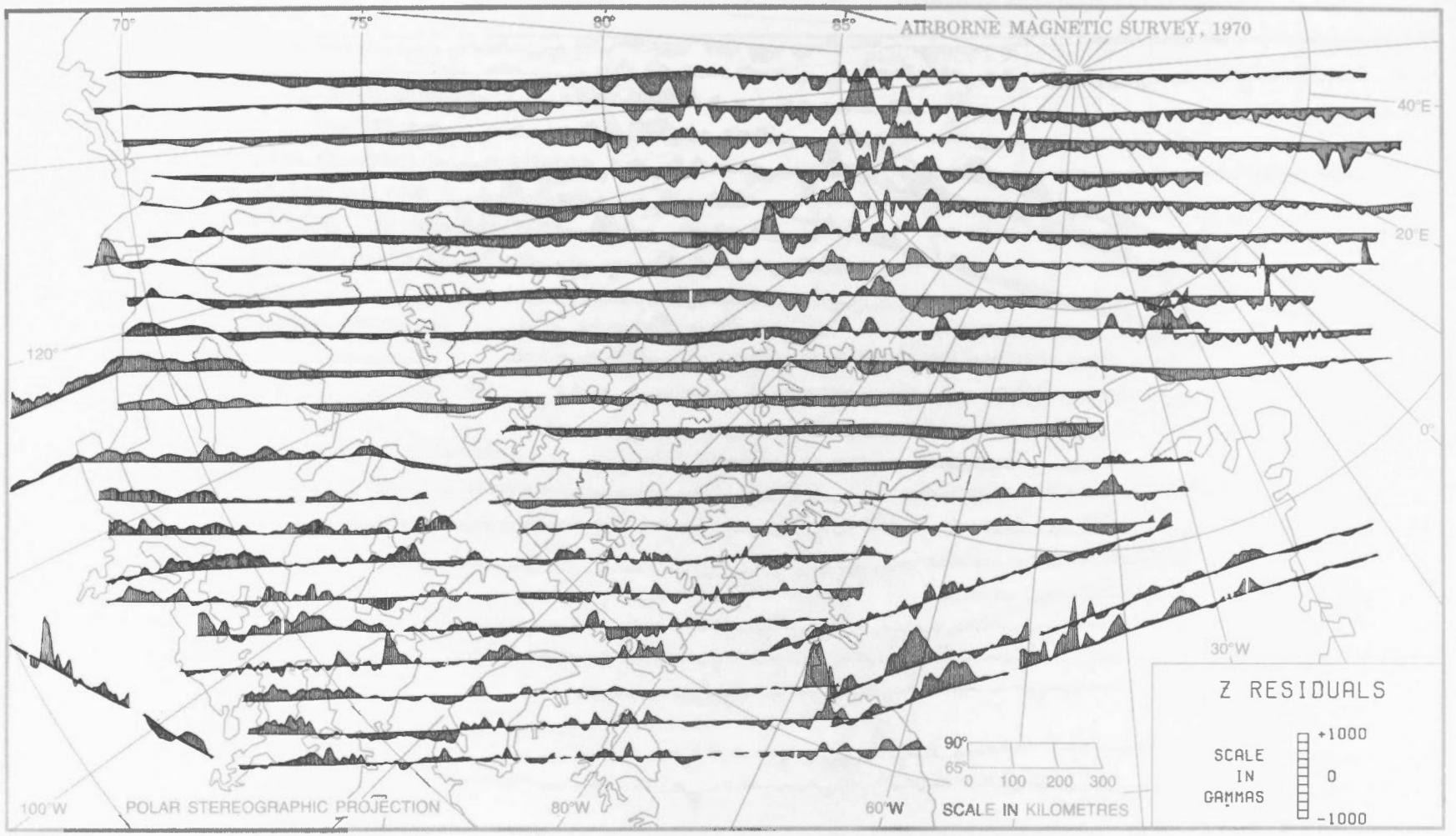

Figure 13. Residual profiles of vertical intensity, relative to the IGRF. Because of the high geomagnetic latitude of the area, total intensity residuals would be practically identical to these.

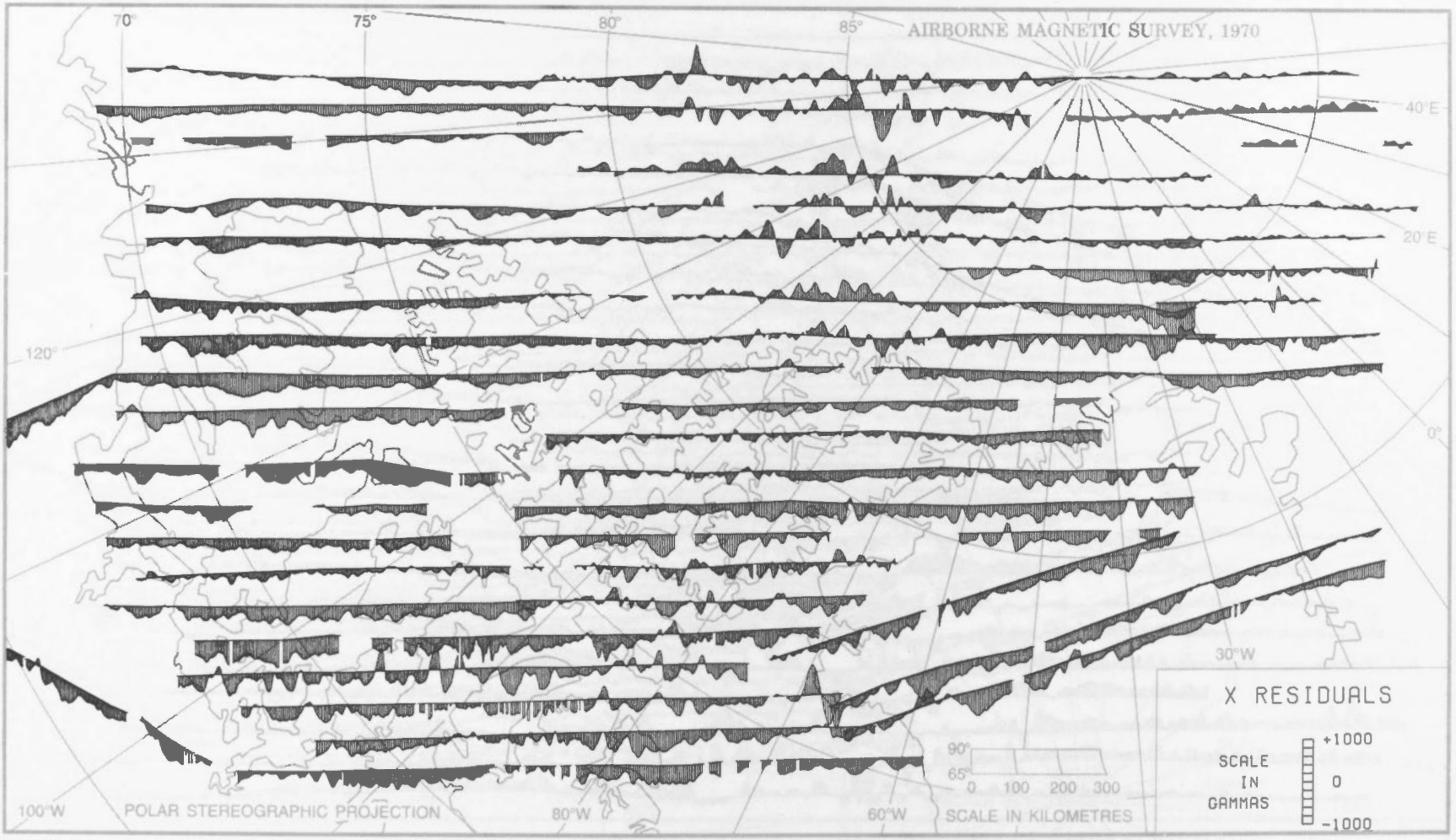

Figure 14. Residual profiles of the geographic north component, relative to the IGRF.

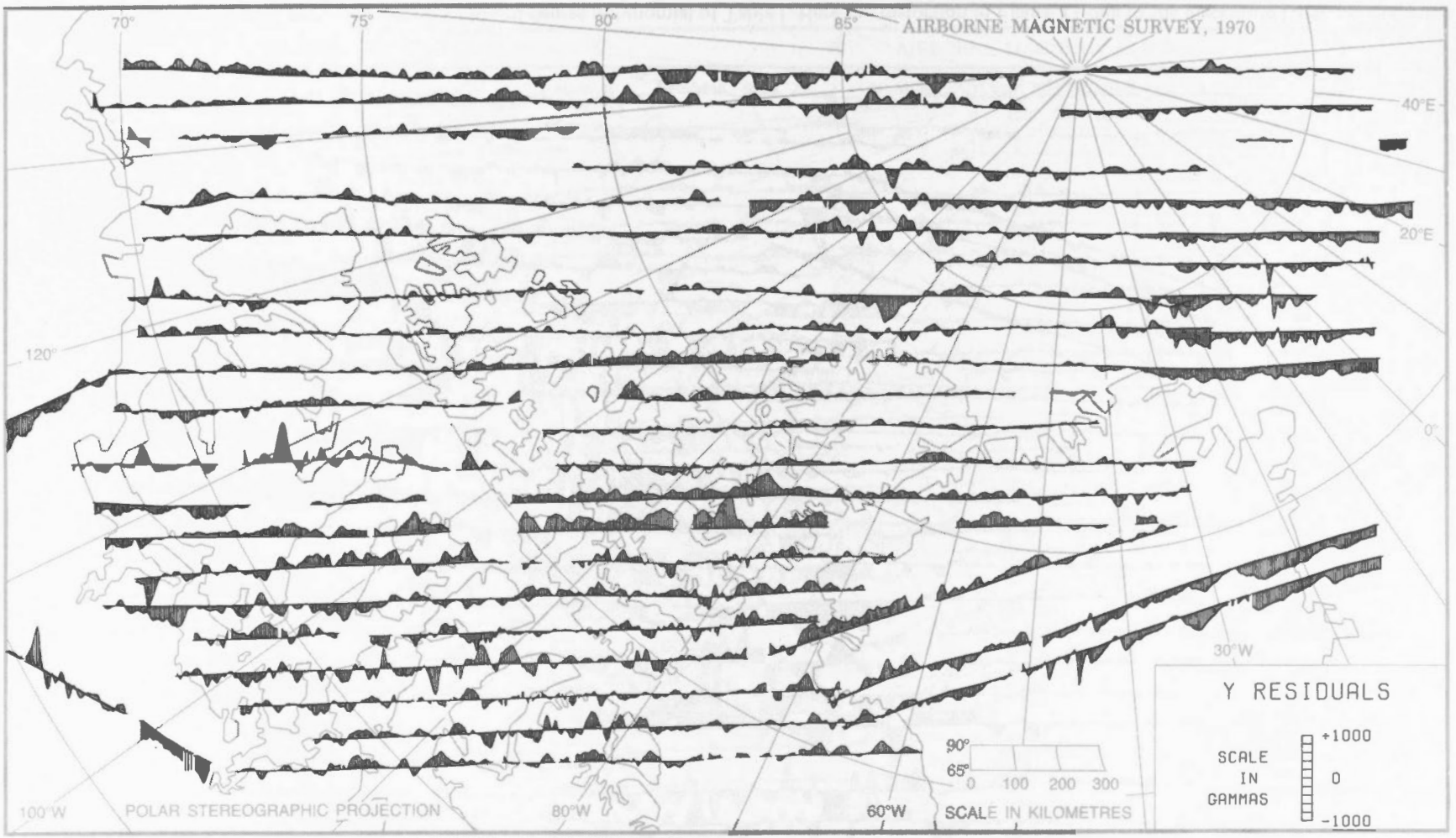

Figure 15. Residual profiles of the geographic east component, relative to the IGRF.

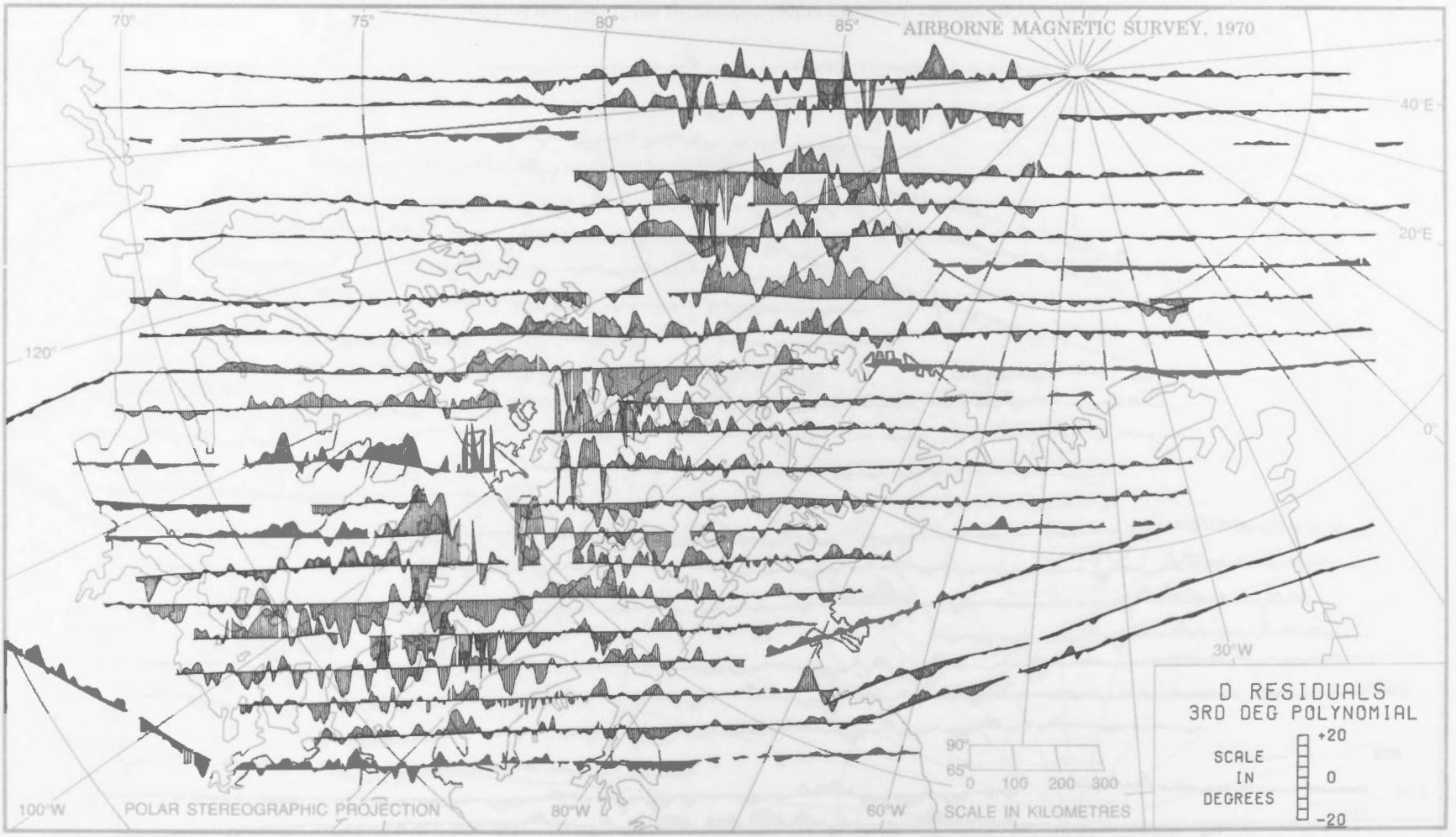

Figure 16. Residual profiles of declination, relative to 3rd-degree polynomial of Table I. Here the distortion in Figure 11 due to the inaccurate IGRF pole position has been removed.

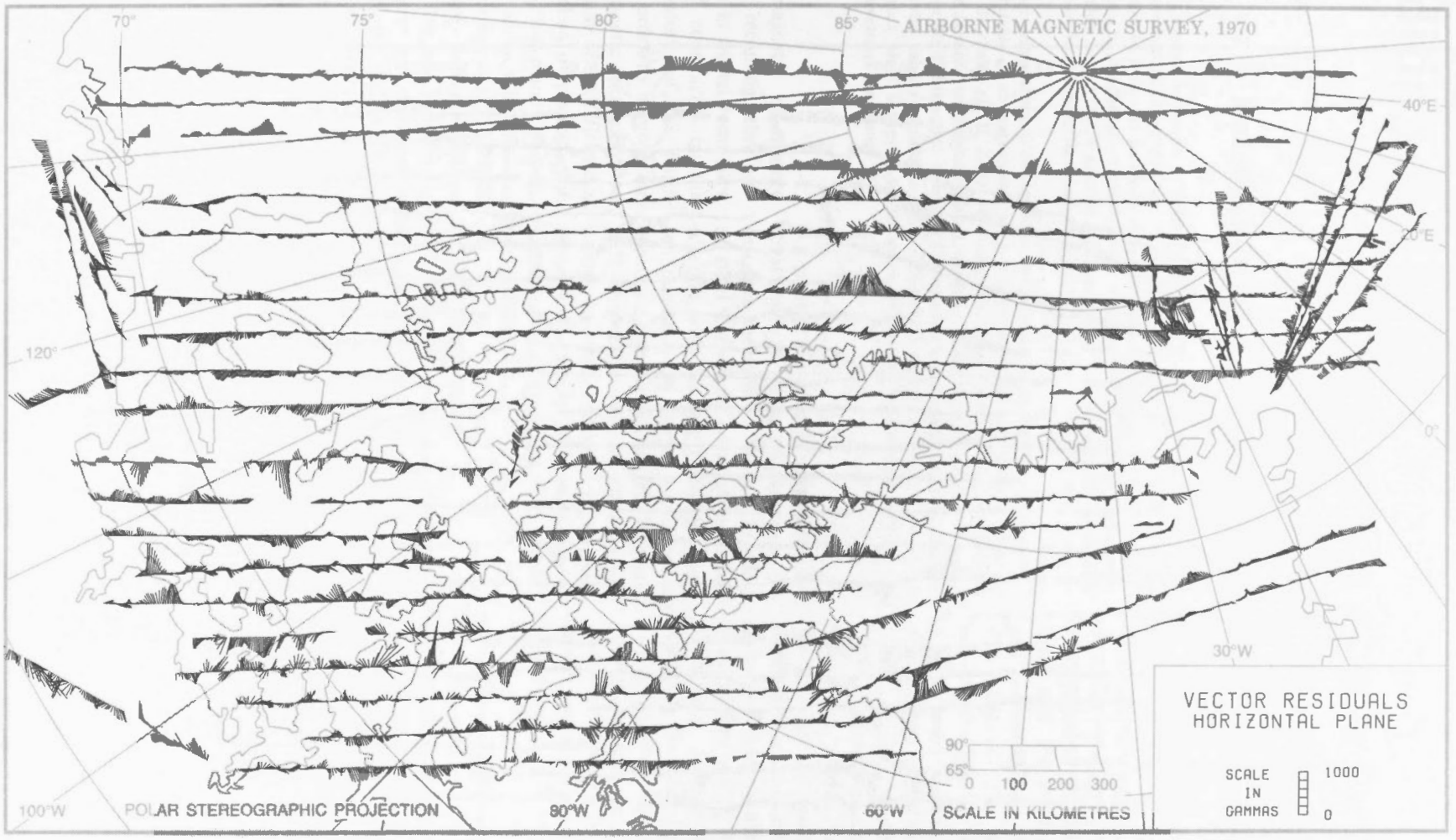

Figure 17. Projection of total residual vector onto horizontal plane. Residual vector is taken relative to 3rd-degree polynomial. Components of vector are plotted toward the top and right of map when positive, toward the bottom and left when negative.

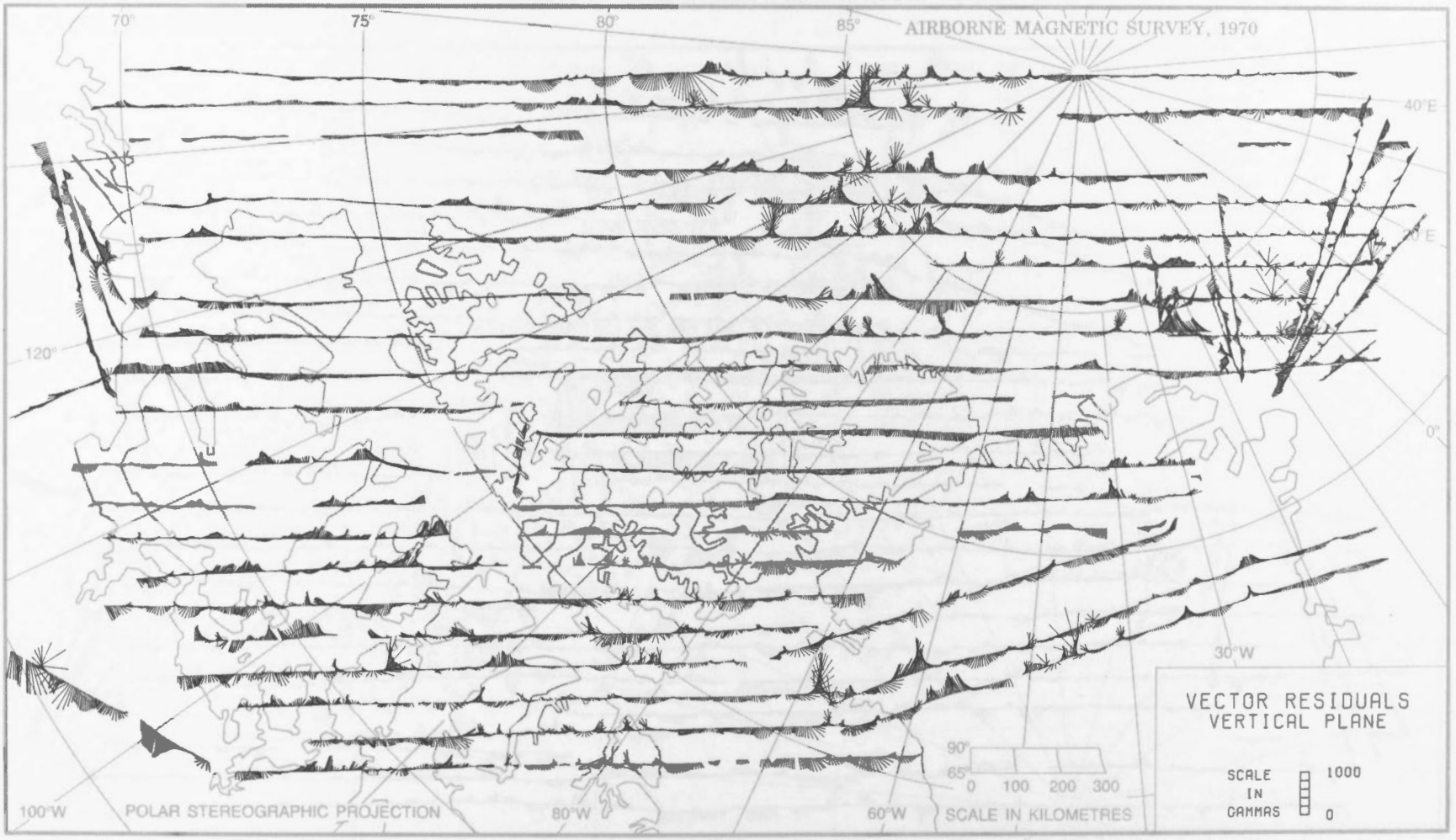

Figure 18. Projection of total residual vector onto vertical plane parallel to x-axis (from left to right, in figure). Residual vector is relative to 3rd-degree polynomial.